View Article Online / Journal Homepage / Table of Contents for this issue
Dynamic Article Links

Journal of Materials Chemistry

Cite this: J. Mater. Chem., 2012, 22, 1762

www.rsc.org/materials

COMMUNICATION

Complete structural model for lanthanum tungstate: a chemically stable high temperature proton conductor by means of intrinsic defects †

Anna Magrasó,*[a] Jonathan M. Polfus,[a] Carlos Frontera,[b] Jesús Canales-Vázquez,[c] Liv-Elisif Kalland,[a] Charles H. Hervoches,[a] Skjalg Erdal,[a] Ragnhild Hancke,[a] M. Saiful Islam,[d] Truls Norby[a] and Reidar Haugsrud[a]

Received 4th October 2011, Accepted 29th November 2011
DOI: 10.1039/c2jm14981h

Published on 14 December 2011. Downloaded by University of Bath on 19/09/2014 13:48:14.

This is the first paper reporting that lanthanum tungstate, earlier believed to be La_6WO_{12}, is in fact $La_{28-x}W_{4+x}O_{54+\delta}$, where tungsten dissolves in lanthanum sites to form a stable solid-state electrolyte, exhibiting proton conduction by hydration at intermediate temperatures.

Oxides that exhibit significant protonic conductivity at elevated temperatures are promising candidates for use as electrolytes in proton conducting fuel cells, while ambipolar conductors can be used as dense ceramic membranes for hydrogen separation in carbon capture processes or fuel upgrading. What was earlier believed to be the hexalanthanum tungstate (La_6WO_{12}) exhibits pure ionic or mixed ionic-electronic conductivity depending on temperature, atmosphere, and the exact La/W ratio.[1–3] The total conductivity is 2–7 mS cm^{-1} at 800 °C, and 0.02–0.03 S cm^{-1} at 1100 °C in wet H_2. Recent investigations have shown that La_6WO_{12} is unstable and leads to an incorrect description of the unit cell.[3] The material is stable only in a window of La/W ratios below 6,[3–5] and single phase materials can only be obtained for compositions with a nominal La/W atomic ratio between 5.3 (labeled LWO53) and 5.7 (LWO57), after firing at 1500 °C.[3] The final annealing temperature is important, as the stability window of composition is temperature-dependent.[3] So, what is the detailed structure that facilitates stabilization, that explains why only off-stoichiometric La/W ratios well below 6 are stable, and that yields a defect model that helps rationalize the transport, doping and hydration behaviour?

Attempts on detailed descriptions of the crystal structure are limited to ref. 3 and 4. The model from ref. 3, represented by a $La_{26.5}W_{4.7}O_{52.8}v_{11.2}$ unit cell (*cf.* Fig. S4 †), was in good agreement with X-Ray Diffraction (XRD), neutron diffraction data, density and chemical microanalyses, and is closely related to Y_7ReO_{14} ($Y_{28}Re_4O_{56}$ unit cell).[6] The structure from ref. 3 had two main challenges still to be solved: first, ~20% of the tungsten was not located with confidence in the structure. Second, W was reported to be 8-fold-coordinated, which was not sufficiently discussed in view of its small size with respect to this coordination. Re(VII) was also reported to be 8-fold coordinated to oxygen in Y_7ReO_{14},[6] but the authors emphasized that it should only be seen as a reasonable description of an averaged high symmetry structure. An interpretation of ReO_8 as two disordered ReO_4 tetrahedra was challenged by too-long Re–O bonds and oxygen site occupancy being significantly higher than 50%. Both arguments can be applied to our lanthanum tungstate as well. An additional challenge with respect to the structure of lanthanum tungstate is related to the amount of empty and filled oxygen sites. The water uptake due to hydration of oxygen vacancies was below 10%,[2,3] which is much lower than expected from the total amount of vacancies in $La_{26.5}W_{4.7}O_{52.8}v_{11.2}$. These aspects are revised in our new structural model. Hence, substantial effort has been devoted to finding the *formula unit* to serve as a parent structure for a defect chemical model. We will first describe the model obtained from computational tools, and afterwards validate it with experimental diffraction techniques.

All final calculations were performed by DFT (within the VASP code),[7] while atomistic techniques by interatomic potentials (within the GULP code)[8] were used to explore a broader range of atomic configurations. The cation positions in the relaxed cells were very close to the sites defined previously, *i.e.* La1(4a), La2(24g) and W(4b) (from $F\bar{4}3m$),[3] and are in agreement with the synchrotron data (to be described later). The interstitial tungsten positions described in ref. 3 were disregarded based on total energy considerations after preliminary computational studies.

First of all, both DFT and potential-based simulations show that the most stable oxygen configuration around W was an octahedron with oxygen sites lying in the vicinity of the corners of the WO_8 cube described in ref. 3. This is in accordance with preliminary results from Raman spectroscopy, which also indicate that W is in an octahedral coordination (typical W–O distances ≈1.9 Å), rather than tetrahedral (~1.7 Å). Furthermore, in the lowest energy configurations, the WO_6 octahedra are oriented in different directions as to give more uniform oxygen coordination around the La1 and La2 sites. La1 sites are generally 8-fold coordinated in regular cubes, while La2 sites are generally coordinated by 7 oxygens in highly distorted cubes.

[a]*Dept. Chemistry, University of Oslo, FERMiO/SMN, Gaustadalleen 21, NO-0349 Oslo, Norway. E-mail: a.m.sola@smn.uio.no; Tel: +47-2284066*
[b]*Inst. Ciència de Materials de Barcelona, ICMAB-CSIC, E-08193 Bellaterra, Spain*
[c]*Renewable Energy Research Institute, University of Castilla-La Mancha, Paseo de la Investigación 1, 02071 Albacete, Spain*
[d]*Dept. Chemistry, University of Bath, Bath, BA2 7AY, UK*

† Electronic supplementary information (ESI) available: Experimental details, additional models by DFT and electrical conductivity. See DOI: 10.1039/c2jm14981h

This journal is © The Royal Society of Chemistry 2012

View Article Online

Published on 14 December 2011. Downloaded by University of Bath on 19/09/2014 13:48:14.

DFT-based molecular dynamics simulations at 1473 K show that the oxide ions are mobile and move along a cube-like frame around W. This suggests that the WO_6 octahedron may reorient or flip in many directions at high temperatures. Thus, while the local environment around the cations is octahedral, the average structure can be represented as a cubic environment due to both the different orientations of the octahedra (space average) and flipping of the octahedra (time average).

The measured La/W ratio, materials' density and lattice parameters enforce higher W content in the unit cell than that corresponding to La/W = 7 ($La_{28}W_4O_{54}$; LWO70).[3] DFT and potential-based calculations showed stable configurations when some W is substituting La on the La2 site, which thus seems to be the way the unit cell accommodates more W ions. The final modelled structure is shown in Fig. 1.

W^{6+} dissolving on La^{3+} sites may initially seem counter-intuitive considering the large difference in size between the two. However, the La2 site has a distorted environment, which was found to be flexible to substitution by W, resulting in $W_{La2}O_6$ octahedra with bond lengths almost identical to the regular W_W–O distance. W_{La2} resides very close to the original La2 position which, in addition to the low fraction of W_{La2} in the overall cell, means that this cation may not be easily differentiated from La2 in diffraction techniques. To further support the presence of W_{La2} defects, it was reported that the lattice parameter had a linear dependence with the La/W nominal ratio, and it was also suggested that phases with lower La content might be stable at lower temperatures.[3] This likely reflects the temperature dependence of the solubility of W in the La2 site.

A variety of high resolution diffraction experiments, including synchrotron, neutron and electron diffraction, have been performed to assess the validity of the structural model described above. The experiments were conducted for the end members of the solid solution after firing at 1500 °C. LWO53 can be indexed as the cubic cell reported previously,[3] but the SPD pattern of LWO57 shows additional (very weak) reflections right beside the peaks stemming from the cubic structure (see the inset in Fig. 2). These small peaks exhibit a full width at half maximum much wider than the main ones. Introducing a secondary phase did not sufficiently improve the refinement, and the peaks may then appear due to a small deviation from the cubic metric. Tetragonal and rhombohedral cells were tested, both giving satisfactory agreement factors, where all the peaks can be indexed and no extra reflection conditions can be identified. The best refinements of SPD data ($\chi^2 = 2.8$; $R_B = 6.9\%$) have been

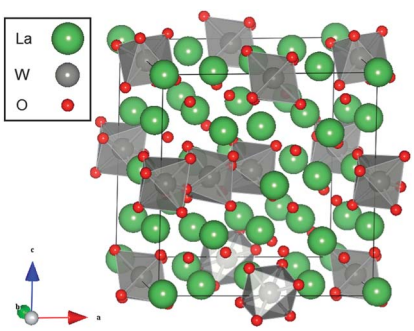

Fig. 1 Relaxed structure of a $La_{28-x}W_{4+x}O_{54+\delta}v_{2-\delta}$ ($x = 1, \delta = 1.5$) unit cell. It shows one W replacing La2 ($x = 1$), and various orientations of tungsten octahedra.

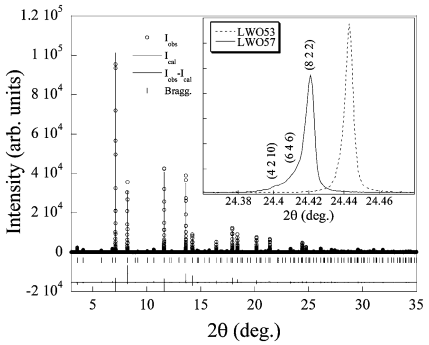

Fig. 2 Rietveld refinement of the SPD pattern of LWO57. The inset shows the splitting of the (10 6 2) cubic reflection into 3 peaks. The same reflections for LWO53 are shown.

obtained using the *I*4/*mmm* space group (no. 139, maximal subgroup of $Fm\bar{3}m$). The body centered tetragonal cell has two formula units per cell, $a_t = a_c/\sqrt{2}$, and $c_t \approx a_c$ (where a_c, a_t and c_t denote the cubic and tetragonal cell parameters). The refined diffractogram is shown in Fig. 2.

It is worth emphasizing that the relative deviation from the cubic cell is very small, around 2.5×10^{-4}, and that such a deviation cannot be detected using laboratory XRD or high-resolution NPD (in both cases $\Delta d/d$ is above 10^{-3}). It is also important to mention that the peaks in SPD patterns from the X-ray synchrotron source for both LWO53 and LWO57 are extremely narrow, and this implies that the cation sublattice is very well defined. As per definition, the content of the tetragonal I-centered cell ($Z = 2$) is half of the cubic F-centered cell ($Z = 4$), but we will, for the discussion, consider the content of two unit cells ($Z = 4$). Rietveld refinements for $La_{28}W_4O_{54}$ (no W at La position) and $La_{27}W_5O_{55.5}$ (one W_{La2}) give rise to the same agreement factor, *i.e.* W occupies the same position as La2 and they are barely distinguishable by X-ray diffraction at such a small substitution level.

The fact that LWO57 (more lanthanum, more vacancies) shows a higher distortion from the cubic cell than LWO53 (more tungsten, less vacancies) may be ascribed to a higher concentration of oxygen vacancies in the former, in accordance with the newly proposed unit cell. The pattern from neutron diffraction is, by far, more difficult to refine than the SPD pattern. This means that oxygen positions are less confined to the positions constrained by the space group and, therefore, more difficult to locate at specific positions in the lattice. Since these oxide ions (and oxygen vacancies) are disordered, the refinement of the average structure becomes even more challenging. The DFT and potential-based calculations (Fig. 1) indicate that it may not be possible to find a space group that can fit the structure at the local level, especially regarding the oxygen environment around tungsten. In any case, the tetragonal and the cubic cells are close descriptions of the average structure of this material.

SAED patterns and HRTEM images down the main zone axes apparently agree with the $F\bar{4}3m$ cubic unit cell previously described in the literature,[3] as most of the main reflections can be indexed according to the space group, though they match *I*4/*mmm* equally well (Fig. 3). Nevertheless, subtle structural differences are detected according to the electron diffraction patterns. Diffuse scattering from slight disorder—probably from oxygen vacancies—has been detected in the W-richer phase (LWO53) along the $[111]_t$ direction, whereas the LWO57 does not show evidence of diffuse scattering in the same

View Article Online

Published on 14 December 2011. Downloaded by University of Bath on 19/09/2014 13:48:14.

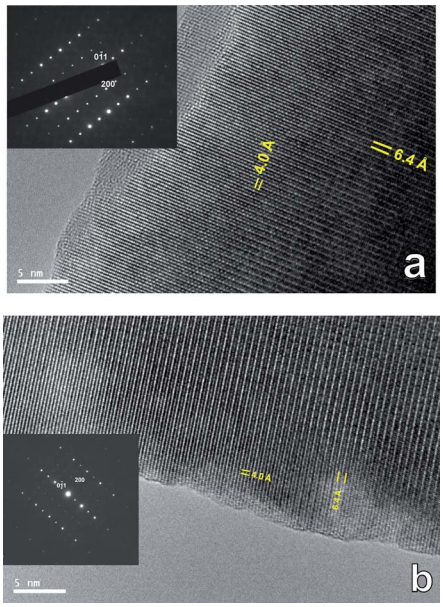

Fig. 3 HRTEM micrographs and the corresponding SAED patterns showing a view down the [011] zone axis for (a) LWO53 and (b) LWO57. Diffuse scattering can be detected in the W-richer composition (a).

zone axis (insets of Fig. 3). This result suggests that the subtle distortion from the cubic symmetry observed from synchrotron data is real and apparently involves a certain degree of oxygen vacancy ordering at local scale for LWO57, similar to that found in some other good oxide-ion conductors such as ceria or zirconia.[9,10] For LWO53 the oxygen vacancies are not ordered and give rise to an average "cubic" unit cell, whereas for LWO57, they may start to cluster and get ordered analogously to C-type Ln_2O_3 structures. This correlates well with our model, since LWO53 has higher tungsten content and therefore fewer vacancies than LWO57. We should also stress that the ordering described here may not occur in the long range, because longer-range ordering would imply the presence of superstructure reflections in the SAED pattern.

The structure that we propose implies that this material can be described with the formula $La_{28-x}W_{4+x}O_{54+\delta}v_{2-\delta}$, where v represents empty oxygen sites. The substitutional W in amounts defined by x possesses effective positive charge and serves as a donor which will be compensated by an increased oxygen content defined by δ. We find that x lies between 0.74 (for LWO57) and 1.08 (for LWO53). Thermogravimetric analysis of LWO56 as a function of temperature and pO_2 reveals that the material does not go through any measurable stoichiometry change between 1100 and 300 °C. This is in support of X-Ray Photoelectron Spectroscopy, which indicates that only W^{6+} is present. Consequently, the defect W_{La2} has an effective charge of 3+ (*i.e.* $W_{La2}^{\cdots}$) and it follows that $\delta = 3x/2$. Atomistic potential-based modelling suggests that the structure is more stable with lower oxygen vacancy concentration *i.e.* lower La/W ratio. This explains why the composition $x = 0$ (La/W = 7: LWO70, $\delta = 2$, v/O = 1/28) is not stable and cannot be synthesized; it may only be achieved at very high temperatures, where structures with more vacancies tend to stabilize due to entropy contributions. Then, when the La/W ratio is decreased and the oxygen sublattice consequently filled, the compound becomes stable and can be prepared.

It is important that the structural model described here can be correlated to its properties. In this direction, we may mention that the water uptake of LWO56, using the new structural model as the parent structure, corresponds to filling ~2/3 of the available oxygen vacancies. This is much higher than that reported before (below 10%), due to overestimating the amount of available oxygen vacancies when tungsten is assumed to be 8-fold coordinated. Also, the La/W ratio in lanthanum tungstate has a measurable impact on the conductivity (*cf.* Fig. S6 †). The W on the La site (W_{La2}) acts as a donor, which is mainly compensated by oxide ions, *i.e.* filling the oxygen vacancies. Therefore, more W inhibits ionic conductivity due to a lower concentration of oxygen vacancies.[11]

To conclude, the structural model derived from a combination of computational modeling and experimental approaches describes a crystal structure that explains the solubility of tungsten on the lanthanum site, and why the material requires lanthanum deficiency to be stable. The properties of the material, such as water uptake and conductivity characteristics, can be rationalized from the expected amount of empty oxygen sites and the consequent defect chemical model, which will be treated in more detail in separate contributions.

Acknowledgements

Authors thank M. S. Sunding and A. Matic for XPS and Raman spectroscopy measurements and Institut Laue Langevin and European Synchrotron Radiation Facility for the provision of beam time. Support from the nanoPCFC, NITROX, HYDROX and KINOXPRO projects of the Research Council of Norway and the NOTUR supercomputer infrastructure in Norway is gratefully acknowledged.

References

1 T. Shimura, S. Fujimoto and H. Iwahara, *Solid State Ionics*, 2001, **143**, 117–123.
2 R. Haugsrud, *Solid State Ionics*, 2007, **178**, 555–560.
3 A. Magrasó, C. Frontera, D. Marrero-López and P. Núñez, *Dalton Trans.*, 2009, 10273–10283.
4 A. Lashtabeg, J. Bradley, A. Dicks, G. Auchterlonie and J. Drennan, *J. Solid State Chem.*, 2010, **183**(5), 1095–1101.
5 C. Solís, S. Escolástico, R. Haugsrud and J. M. Serra, *J. Phys. Chem. C*, 2011, **115**(22), 11124–11131.
6 H. Ehrenberg, T. Hartmann, K. G. Bramnik, G. Miehe and H. Fuess, *Solid State Sci.*, 2004, **6**, 247–250.
7 G. Kresse and J. Furthmuller, *Phys. Rev. B: Condens. Matter Mater. Phys.*, 1996, **54**, 11169.
8 J. D. Gale, *J. Chem. Soc., Faraday Trans.*, 1997, **93**, 629–637.
9 S. García-Martín, M. A. Alario-Franco, D. P. Fagg, A. Feighery and J. T. S. Irvine, *Chem. Mater.*, 2000, **12**, 1729.
10 F. Ye, T. Mori, D. Ou, J. Zou and J. Drennan, *Mater. Res. Bull.*, 2007, **42**(5), 943–949.
11 S. Erdal, L.-E. Kalland, R. Hancke, J. Polfus, R. Haugsrud, T. Norby and A. Magrasó, *Int. J. Hydrogen Energy*, 2011, DOI: 10.1016/j.ijhydene.2011.11.093, in press.

 This journal is © The Royal Society of Chemistry 2012